Emission characteristics and dynamics of the stagnation layer in colliding laser produced plasmas

P. Hough,[1,a)] C. McLoughlin,[1] S. S. Harilal,[2] J. P. Mosnier,[1] and J. T. Costello[1]
[1]*School of Physical Sciences and National Centre for Plasma Science and Technology (NCPST), Dublin City University, Glasnevin, Dublin 9, Ireland*
[2]*School of Nuclear Engineering, Purdue University, 400 Central Drive, West Lafayette, Indiana 47907, USA*

(Received 22 September 2009; accepted 26 November 2009; published online 25 January 2010)

The expansion dynamics of ion and neutral species in laterally colliding laser produced aluminum plasmas have been investigated using time and space resolved optical emission spectroscopies and spectrally and angularly resolved fast imaging. The emission results highlight a difference in neutral atom and ion distributions in the stagnation layer where, at a time delay of 80 ns, the neutral atoms are localized in the vicinity of the target surface (<1 mm from the target surface) while singly and doubly charged ions lie predominantly at larger distances, <1.5 and <2 mm, respectively. The imaging results show that the ions were found to form a well defined, but compressed, stagnation layer at the collision front between the two seed plasmas at early times ($\Delta t < 80$ ns). On the other hand, the excited neutrals were observed to form a V-shaped emission feature at the outer regions of the collision front with enhanced neutral emission in the less dense, cooler regions of the stagnation layer. © *2010 American Institute of Physics*. [doi:10.1063/1.3282683]

I. INTRODUCTION

Laser-produced plasmas (LPPs) have been the focus of substantial research interest since their discovery in the 1960s[1] and have spawned a wide range of applications including material composition analysis [laser induced breakdown spectroscopy (LIBS)],[2] pulsed laser deposition (PLD),[3] and tabletop sources of short wavelength light.[4] Indeed new and emerging areas of applications for LPPs including ion accelerators,[5] high harmonic generation,[6] and laboratory simulations of astrophysical plasmas[7] have provided an even greater impetus to research into the area in recent years. A long established but yet to be fully exploited subdomain of laser-plasma research concerns colliding LPPs. It shows much promise for the future in areas such as thin film deposition. For example, recently droplet-free films were successfully fabricated using colliding laser produced plasmas.[8] It has also been shown[9,10] that heating of a preformed plasma with an intense laser pulse has the ability to increase laser absorption and consequently provide emission intensity enhancement. This has led to benefits in the area of LIBS, for example, where prepulsing has been shown to enhance analyte line emissions.[11] Since the stagnation layer is itself a preheated slab of plasma, it can at least be speculated that it could be used as a source for similar applications.

Significant work has been carried out on high-energy colliding plasmas with laser intensities $\sim 10^{14}$ W cm^{-2},[12] especially, but not exclusively on indirect drive fusion.[13] In indirect fusion devices, a hollow hohlraum hosts multiple colliding plasmas as x-ray sources, which are used to drive fusion in a fuel cell located at the center of the hohlraum.[14] Colliding plasmas have also shown much potential as laboratory scale models of astronomical interactions between colliding shock waves where, for example, Gregory *et al.*[15] and Smith *et al.*[16] showed how they can be used as a scaled model of astrophysical colliding shocks.

When two plasmas collide, under appropriate conditions, as outlined by Rambo *et al.*,[17] a layer of stagnated plasma is formed at the collision front between the two counterpropagating plasmas. Outside these conditions the colliding plasmas undergo interpenetration where the plasmas pass through each other without stagnating. Rambo *et al.* introduced the so called "collisionality parameter," ξ, to determine whether stagnation or interpenetration will dominate in colliding plasmas. The collisionality parameter is given by

$$\xi = \frac{L}{\lambda_{ii}},$$

where L is the typical plasma dimension (i.e., the separation between the two colliding plasmas) and λ_{ii} is the ion-ion mean free path given by[18]

$$\lambda_{ii} = \frac{m_i^2 v_{12}^4}{4\pi e^4 Z^4 n_i \ln \Lambda_{12}},$$

where m_i is the ion mass, v_{12} is the relative collision velocity in the charge of the electron, Z is the average ionization state of the plasma, n_i is the average plasma ion density, and $\ln \Lambda_{12}$ is the so-called Coulomb logarithm[19] for collisions between seed plasma 1 and seed plasma 2. Inserting values of plasma parameters typical of our experiments ($n_i = 10^{17}$ cm^{-3}, $Z=2$, $v_{12}=4\times 10^6$ cm s^{-1}) we obtain a value of 27 for the collisionality parameter and so our plasmas are firm in the medium-low collisionality regime.[17]

The physical process of stagnation layer formation has been found to be very complex. For example, Pollaine *et al.*[20] showed that plasma stagnation can be preceded by a phase of interpenetration where the plasmas initially pass through each other. Rancu *et al.*[21] also found how interpen-

a)Electronic mail: padraighough@gmail.com.

etration and stagnation in colliding laser exploded Al/Al and Al/Mg foils are highly dependent on the collisionality parameter. We have previously shown[22] that separation of charge in space can play a significant role in stagnation of various plasma constituents.

With many simultaneous and complex processes involved, it is critical that comprehensive diagnostics of the plasmas and the stagnation layer are performed in order to obtain a more complete picture of the physical nature of colliding plasmas. Comprehensive diagnostics can also provide extremely useful reference data for colliding plasma modeling efforts[23] especially for colliding plasmas in the medium to low collisionality regime. There is thus a great need for experimental data on both the structure and dynamics of colliding laser produced plasmas and we aim to address this issue here by employing angularly resolved fast imaging and OES to extract more detailed information on the atom and ion distributions and evolution in the stagnation layer.

In an earlier paper, we concentrated on the time correlation between electron and ion stagnation using interferometric and fixed angle optical imaging as the relevant diagnostic techniques.[22] Our emphasis was on the nascent phase of stagnation layer formation (i.e., <20 ns). The present study is focused on imaging the stagnation layer at relatively early (≈ 80 ns) and late (≈ 150 ns) times in its lifecycle (relative to the overall lifetime of the stagnation layer). In addition, to our knowledge, angle resolved measurements of the interaction occurring at the collision plane have only been the subject of interferometric studies to date.[24] In this report, we focus on obtaining information about the distribution of atoms and ions in the stagnation layer using the angularly resolved optical imaging technique. At the collision plane between two counterpropagating plasmas, a new brightly emitting region (i.e., the stagnation layer) is created whose characteristic volume or shape depends strongly on the original seed plasma properties. Our results indeed show that the emission features vary with angle of view for certain plasma species. Such data reveal the detailed structure of the layer in multiple expansion axes and the diagnostic technique will prove useful for the study of systems using other colliding plasma geometries. We have also employed optical emission spectroscopy (OES) as a complementary tool for analyzing the spatiotemporal distributions of various plasma constituents.

II. EXPERIMENT

The optical system used to split the laser beam and create the colliding laser produced plasmas is similar to that used by Harilal *et al.*[25] A 0.5° wedge prism used in combination with a 30 cm focal length plano-convex lens split a neodymium-doped yttrium aluminum garnet laser beam [1064 nm, 600 mJ, 6 ns full width at half maximum (FWHM)] into two parts. The two foci created at the target plane with spot diameters of ~ 100 μm were separated by a distance of 1.3 mm. The laser beam was incident normal to the target surface. The target was a flat slab of 99.99% pure aluminum mounted on a high precision in vacuum X-Z motorized stage which was used to reveal a fresh surface after each laser shot. The pressure in the chamber was maintained at better than 1×10^{-5} mbar for all experiments presented here.

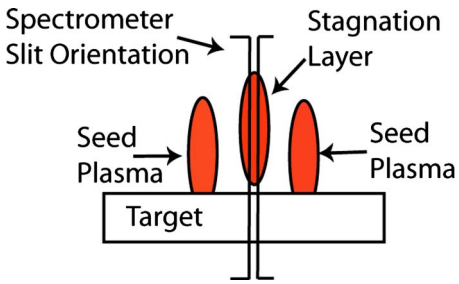

FIG. 1. (Color online) Illustration of the orientation of the spectrometer slit with respect to the stagnation layer. This arrangement provided one-dimensional spatial resolution normal to the target along the stagnation layer.

The optical system used to perform the OES studies is similar to that used by Doria *et al.*[26] An intensified charged coupled device (ICCD) (Andor Technology, 1024 $\times$ 1024 pixels with a pixel size of 13×13 μm^2) was employed to perform the spatially and temporally resolved OES measurements. The camera was mounted on a Chromex 0.5 m optical 1:1 imaging spectrometer with a 1200 l/mm grating resulting in a wavelength resolution of 0.1 nm. The plasma was imaged onto the slit of the spectrograph using achromatic imaging lenses with a magnification of 2×. Figure 1 illustrates the orientation of the slit of the spectrometer with respect to the stagnation layer. The spectrometer was used to analyze line emission from neutral, singly, and doubly charged aluminum. The slit width was set to a width of 60 μm and all spectra were averaged over 10 laser shots. The shutter width for each shot was set to 3 ns.

The ICCD camera was also employed to perform fast photography. A telephoto lens, located at right angles to the target surface, was used to image the plasmas onto the ICCD. A gate width of 3 ns was used for obtaining all images. To observe the colliding plasmas with angular resolution, we rotated the wedge prism in order to rotate the colliding plasmas on the target surface, effectively changing our camera's angle of view but without having to adjust the cameras position in any way. In Fig. 2, we define the two angles of view (0° and 90°) used in our fast photography study. The 0° angle

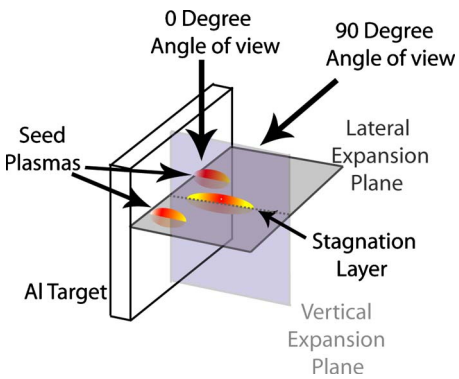

FIG. 2. (Color online) Definition of the viewing angles used for the angularly resolved fast photography with respect to the orientation of the colliding plasmas.

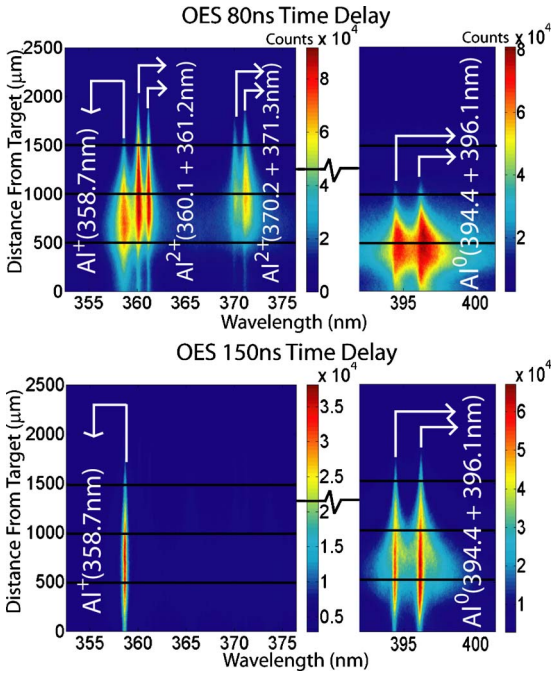

FIG. 3. (Color online) Comparison of the optical spectra obtained showing line emission from neutral, singly, and doubly charged aluminum as a function of distance from the target at two different delay times (80 and 150 ns). The black lines serve to highlight the distances of 0.5, 1, and 1.5 mm from the target surface.

of view observed the stagnation layer in the lateral expansion plane, whereas the 90° angle of view observed the stagnation layer in the vertical expansion plane.

Narrow band spectral filters have been used to select the emission distributions of various plasma species in the stagnation layer. Emission from Al^+ was selected with the aid of a bandpass filter centered at 460 nm which had a full width at half maximum of 10 nm, placed in front of the ICCD camera. For capturing the excited Al neutral species distribution, a narrow bandpass filter centered at 390 nm was used. An edge pass filter was employed to select broadband emission from 300 to 950 nm and also served to block any stray 1064 nm laser radiation. The camera was synchronized with the laser using a Stanford DG535 delay generator which resulted in a maximum temporal jitter of ± 1 ns. Images for neutral and singly charged aluminum atoms were averaged for 3 and 5 laser shots, respectively, while the broadband images correspond to emission from a single laser shot to avoid saturating the camera.

III. RESULTS AND DISCUSSION

A. Spatially resolved OES

Spatially resolved OES provides the intensity distributions of the various species in the stagnation layer. Our spectral studies indicate that the emission features within the stagnation layer mainly comprise of excited neutrals along with the singly and doubly charged ions. Corresponding spectra are shown in Fig. 3 where we compare line emission for neutral, singly, and doubly charged aluminum as a function of distance from the target for two different time delays (80 and 150 ns). In these plasma regimes, the birth of the

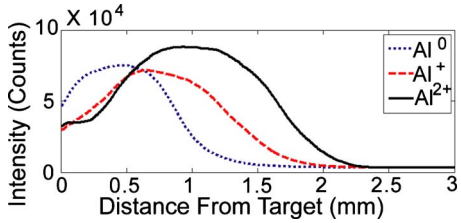

FIG. 4. (Color online) Al^0 (396.15 nm), Al^+ (358.65 nm), and Al^{2+} (360.19 nm) emissions as a function of distance from the target at a delay time of 80 ns providing evidence of the space charge effects.

stagnation layer occurs at a time delay of 20–30 ns or so and it usually dissipates into the surrounding environment at a time delay of ~200 ns. Thus observing the stagnation layer at time delays of 80 and 150 ns will reveal the structure of the layer at relatively early and late times, respectively.

Spectra in the region of 365 nm capture line emission from both singly charged and doubly charged ions. The line at 358.7 nm is a 4f $^3F_3$-3d $^3D_3$ transition in singly charged aluminum. The other lines present in the spectra originate from transitions in doubly charged ions at 360.19 nm (3d $^2D_{3/2}$-4p $^2P_{3/2}$), 361.23 nm (3d $^3D_{3/2}$-4p $^2P_{1/2}$), 370.2 nm (4p $^2P_{1/2}$-5s $^2S_{1/2}$), and 371.31 nm (4p $^2P_{3/2}$-5s $^2S_{1/2}$).[27] This wavelength region is well suited to the task of making a comparison of the spatial distributions of singly and doubly charged ions. From Fig. 3, it is clear that at a time delay of 80 ns (top left panel), the spatial extent of singly charged ions is limited to a region extending out to 1.5 mm from the target surface with the peak of the emission centered around a region lying 0.7 mm from the target. The doubly charged ions, however, can be seen at much larger distances (up to 2 mm) from the target with an emission distribution that peaks at a distance of 1 mm.

The emission from neutral aluminum comprises transitions at 394.4 nm (4s $^2S_{1/2}$-3p $^2P_{1/2}$) and 396.15 nm (4s $^2S_{1/2}$-3p $^2P_{3/2}$). At 80 ns, again looking along the direction normal to the target surface, the neutral-atom distribution is found to be less extended than either the singly or doubly charged ions. In fact, neutral species reach a maximum distance of only ≈1 mm from the target with the peak emission originating from a region lying at a distance of 0.5 mm from the target.

Figure 4 shows a comparison of the spatial distribution of the line emission from Al^0 (396.15 nm), Al^+ (358.65 nm), and Al^{2+} (360.19 nm) at a time delay of 80 ns and clearly highlights the spatial distribution of plasma atomic species along the stagnation layer.

Ursu *et al.*[28] showed how the expansion velocities of the ionized species in single laser produced plasmas are found to increase with the degree of ionization. Not unexpectedly then, excited neutral species were found to be the slowest moving particles[28] (Fig. 4). In their experiment, they also employed an ICCD camera coupled to an optical spectrometer to identify and track over time, line emission for neutral, singly, and doubly charged ions emitted from a single laser produced aluminum plasma. We have already observed[22] the spatial separation of electrons and singly charged ions in the collision plane at very early times (<20 ns) just prior to and during the early phase of stagnation. By utilizing a Nomarski

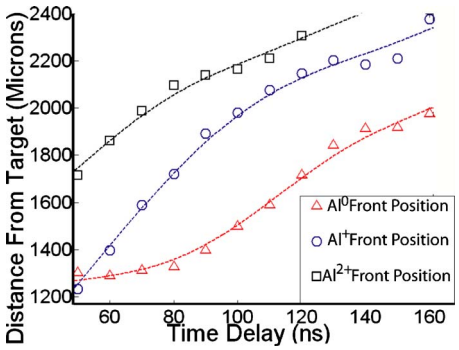

FIG. 5. (Color online) Expansion traces for the luminous front positions of Al^0 (396.15 nm), Al^+ (358.65 nm), and Al^{2+} (360.19 nm) emission emphasizing the differences in the spatial evolution of the three ion stages. The smooth curves are best fitted spline curves.

laser interferometer[29] and comparing with the results from fast imaging, we found that electrons, which are known to be the first plasma constituents to leave the seed plasmas as observed by Okano *et al.*,[30] are the first to stagnate at the interface between two colliding plasmas, followed very closely by the ions.[22] We have also found that ion stagnation precedes neutral-atom stagnation.[31] In the present experiment, however, we see how the development of the stagnation layer, at later times (~80 ns), is most definitely influenced by the mechanisms of expansion in the seed plasmas. Specifically we see emission in the stagnation layer from doubly charged ions lying at the furthest distances from the target, due to the fact that they expand away from the seed plasmas with a larger velocity than either singly charged or neutral atomic species. Similarly emission in the stagnation layer from the singly charged ions predominates at greater distances from the target than the excited neutral species.

At relatively later times (150 ns, Fig. 3, bottom panel) most of the emission originates from neutral atoms and singly charged ions suggesting that the number density of doubly charged ions have declined through recombination processes by this time. The Al atoms and Al^+ ions are observed to emit from very similar regions (at later times) implying that the stagnation layer has developed into a more uniform plasma with neutral atom and ion emission distributed more isotropically.

Figure 5 shows stagnation layer expansion trace (distance versus time) of neutral, singly, and doubly charged aluminum emission obtained from OES. The selected emission lines are 396.15, 358.65, and 360.19 nm for Al^0, Al^+, and Al^{2+}, respectively. The luminous front is defined to be the position of the plasma front where the emission is measured to be 10% of the peak plasma emission. An important note for one to bear in mind is that this trace is indicative of the *spatial development* (normal to the target, see Fig. 2) of various species in the *stagnation layer*. Ions leaving the seed plasmas can travel along many different trajectories and so will reach the stagnation layer in different positions and different times. Hence inferring an "expansion velocity" for any one species in the stagnation layer or indeed the stagnation layer as a whole would be somewhat misleading.

It can be clearly seen from Fig. 5 that the emission front for the neutrals and the two ion stages differ spatially by a substantial amount. The emission front from doubly charged Al extends furthest from the target surface. Similarly the emission front of singly charged aluminum extends farther from the target than neutral aluminum radiation and this observation is maintained over time. To complement these studies, we have employed spectrally resolved ICCD imaging; results are shown in Sec. III B.

B. Angularly, temporally, and spectrally resolved optical fast imaging

Based on the results from the OES study, we have chosen two narrow bandpass filters to select line emission from neutral and singly charged aluminum, thus allowing us to track their individual development in the stagnation region. An optical filter centered at 390 nm (FWHM of 10 nm) was chosen to select neutral atomic aluminum emission [394.4 nm ($4s\ ^2S_{1/2}$-$3p\ ^2P_{1/2}$) and 396.15 nm ($4s\ ^2S_{1/2}$-$3p\ ^2P_{3/2}$)] while a narrow bandpass filter centered at 460 nm (FWHM of 10 nm) was utilized to isolate Al^+ line emission [466.3 nm ($3s4p\ ^1P_o$-$3p^2\ ^1D$)].

Images of colliding plasmas were obtained at two orthogonal camera angles [defined in Fig. 2]. The 0° angle of view is the standard viewing angle for studying colliding laser produced plasmas[25,32] but this method is limited in that it only exposes the emission features of the stagnation layer in the lateral expansion plane (see Fig. 2). Viewing the stagnation layer from the 90° angle of view reveals the structure of neutral atoms, singly charged ions, and whole plasma broadband emission in the vertical plane. The results of this imaging study are shown in Fig. 6. The time delay for each image was 90 ns, by which time the emission from the seed plasmas has faded and so they do not occlude the view of the stagnation layer when observing at the 90° viewing angle. Also included are the normalized lineouts to compare the spatial distributions (parallel to the target) of the atoms, ions, and broadband emission at a distance of 1 mm from the target for the two different viewing angles. The white lines in the images serve to illustrate the locations where the lineouts were taken.

The most prominent feature in Fig. 6 is the asymmetry of the emission from Al^+ in the stagnation layer when looking from the two orthogonal viewing angles. The singly charged ions form a narrow elongated layer of plasma at the interface between the two seed plasmas. Pressure from the two seed plasmas, in the lateral expansion plane (0° angle of view), pinches the stagnation layer at early time delays (<80 ns) when plasma expansion from the seed plasmas is very strong, i.e., when a good deal of plasma material is expanding from the laser produced plasma. It therefore serves to enhance Al^+ expansion in the orthogonal direction (along the vertical expansion axis observed at the 90° angle of view). This is illustrated by the corresponding lineouts (right panel) for the Al^+ emission in Fig. 6. The broadband emission, characteristic of the relevant range of ion stages emitting in the 300–950 nm spectral window, indicates the overall stagnation layer to be quite cylindrically symmetric.

Emission from the neutral atoms displays a somewhat symmetric profile with the lineouts from both viewing angles

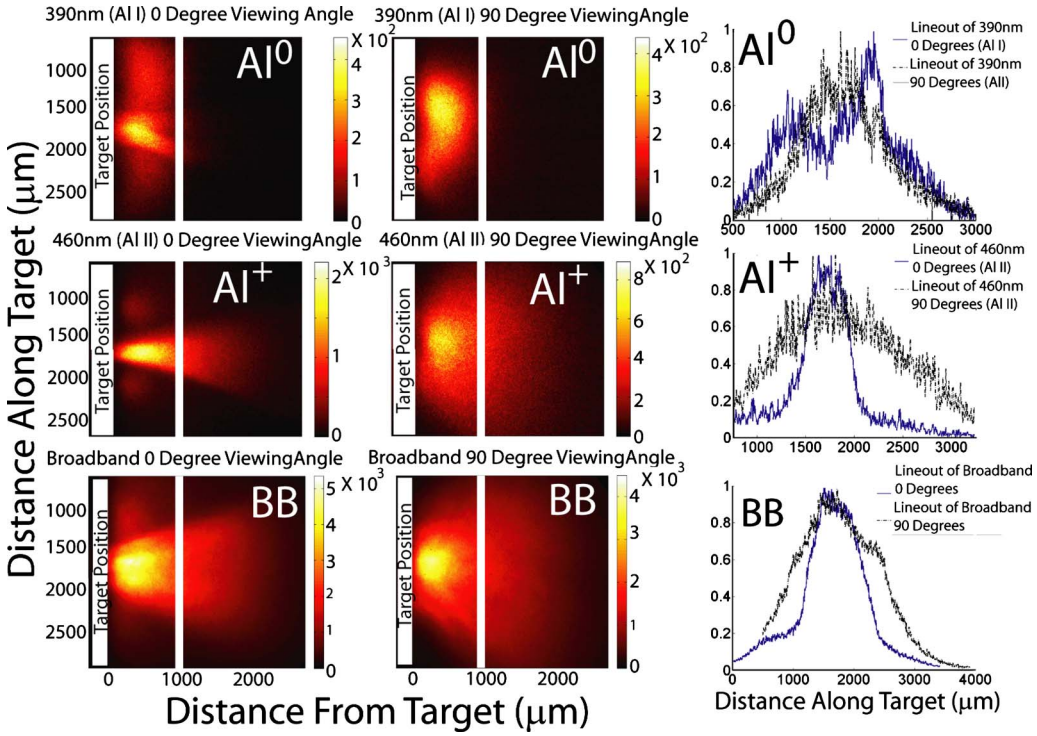

FIG. 6. (Color online) Comparison of the angularly resolved spatial emission from neutral Al atoms with that of singly charged Al ions and broadband emission for the two angles (0°, left panels and 90°, center panels) defined in Fig. 2 (recorded at a delay time of 90 ns). The right hand panel shows the comparison of the emission distribution (lineouts) from the two viewing angles along a line parallel to, but separated from, the target surface by a distance of 1 mm. The white lines in the images show where the lineouts were taken for comparison.

having similar profiles. There is, however, evidence of a nascent V-shaped profile in the image recorded at the 0° viewing angle (see central dip in blue lineout in top right panel). This V-shaped profile is much more prominent at relatively later times (>100 ns), as can be seen in Fig. 7, where the emission images (all taken at 0° angle of view, the lateral expansion axis) of Al^0, Al^+, and whole plasma are given for two delay times (80 and 150 ns). Similar structures were noticed in laterally colliding plasmas previously with x-ray[33] diagnostics. In that study, Farley *et al.* observed high energy colliding plasmas (10^{15} W cm^{-2}) in the x-ray region and found that large radiative losses in the denser central region give rise to a V-shaped emission feature just after plasma formation (1.1 ns).

In our case, the colliding plasmas are in a very different parameter regime and at much later times (80 ns) and so the same reasoning cannot be employed here. We propose that the bifurcation of the neutral emission in Fig. 7 can be explained as follows. The ion stagnation, as already discussed, precedes the arrival of the slower neutral species and hence they do not penetrate the ion stagnation layer to any great degree. Rather they collide preferentially with the outer region of the pinched layer where they emit strongly giving rise to a V-shaped neutral feature; in effect the preformed ion layer acts as a wedge preventing neutral-neutral collisions and the emission observed is due, at least in part, to neutral-atom collisions.

IV. CONCLUSIONS

We have investigated the emission features of excited neutrals and ions in the stagnation layer of a laterally collid-

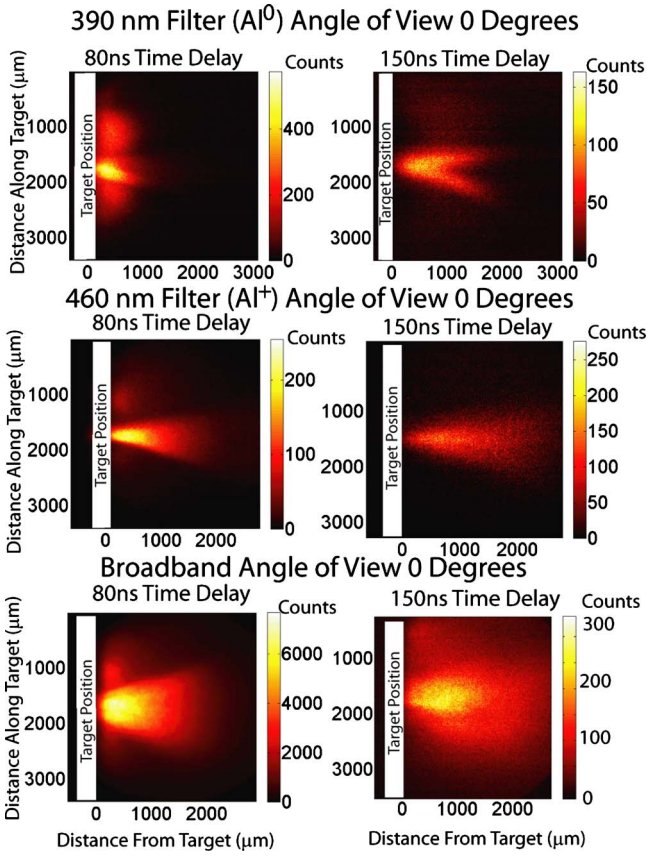

FIG. 7. (Color online) Comparison of emission from Al^0, Al^+, and broadband imaging for a fixed viewing angle (0°) for two different delay times (80 ns, left panels and 150 ns, right panels).

ing laser produced plasma. Angularly, spectrally, and temporally resolved optical imaging and spatially and temporally resolved OESs were used to diagnose the stagnation layer. The OES shows clear differences in the spatial extent of atoms with respect to that of singly and doubly charged ions. Atoms were found to remain closer to the target than ions and doubly charged ions were found to extend further from the target than singly charged ions.

Emission from neutral atoms appeared as a V-shaped distribution extending from the target surface. Angularly and spectrally resolved fast photographies revealed an asymmetric layer of ions in the stagnation layer. This layer is formed very early (<80 ns) in contrast to the atoms (~ 150 ns) at a time when the seed plasma are very prominent, thereby causing compression of the layer. In contrast the broadband and atomic layer emission is quite cylindrically symmetric about an axis normal to the target, however, with a dip in the atomic emission observable at the center in the lateral expansion plane. The study should be very useful in building up a more complete picture of the mechanisms involved in stagnation layer formation and structure for relatively low energy colliding laser-plasma experiments and apposite applications, e.g., PLD. It should also provide a useful reference data set for testing models in this parameter regime of colliding plasmas with a mid-low collisionality parameter.

ACKNOWLEDGMENTS

This work was sponsored by the Science Foundation Ireland under Grant No. PHY041 and the SFI PI Grant No. 07/IN.1/I1771 and the HEA PRTLI IV INSPIRE program of the Second National Development Plan program (NDP2). One of the authors (P.H.) would like to acknowledge support from the Embark Scholarship Scheme of the Irish Research Council for Science Engineering and Technology. S.S.H. acknowledges funding from the DCU International Visiting Fellows Programme. Work is associated with EU COST Action MP0601. The authors wish to thank Des Lavelle for help in the design and construction of the experimental system.

[1]S. A. Ramsden and W. E. R. Davies, Phys. Rev. Lett. **13**, 227 (1964).
[2]C. Pasquini, J. Cortez, L. M. C. Silva, and F. B. Gonzaga, J. Braz. Chem. Soc. **18**, 463 (2007).
[3]R. O'Haire, E. McGlynn, M. O. Henry, and J. P. Mosnier, Superlattices Microstruct. **42**, 468 (2007).
[4]Y. Tao, M. S. Tillack, K. L. Sequoia, R. A. Burdt, S. Yuspeh, and F. Najmabadi, Appl. Phys. Lett. **92**, 251501 (2008).
[5]S. V. Bulanov, T. Z. Esirkepov, F. F. Kamenets, Y. Kato, A. V. Kuznetsov, K. Nishihara, F. Pegoraro, T. Tajima, and V. S. Khoroshkov, Plasma Phys. Rep. **28**, 975 (2002).
[6]R. A. Ganeev, M. Suzuki, M. Baba, and H. Kuroda, Appl. Phys. Lett. **94**, 051101 (2009).
[7]Ph. Nicolaï, V. T. Tikhonchuk, A. Kasperczuk, T. Pisarczyk, S. Borodziuk, K. Rohlena, and J. Ullschmied, Phys. Plasmas **13**, 062701 (2006).
[8]E. Irissou, F. Vidal, T. Johnston, M. Chaker, D. Guay, and A. N. Ryabinin, J. Appl. Phys. **99**, 034904 (2006).
[9]A. Murphy, J. S. Hirsch, D. Kilbane E. T. Kennedy, M. A. Khater, J-P. Mosnier, A. Neogi, G. O'Sullivan, C. L. S. Lewis, S. Topping, R. Clarke, E. Divall, P. Foster, C. Hooker, A. Langley, D. Neely, P. Dunne, and J. T. Costello, Proc. SPIE **4878**, 1196 (2003).
[10]P. Dunne, G. O'Sullivan, and D. O'Reilly, Appl. Phys. Lett. **76**, 34 (2000).
[11]V. I. Babushok, F. C. DeLucia, J. L. Gottfried, C. A. Munson, and A. W. Miziolek, Spectrochim. Acta, Part B **61**, 999 (2006).
[12]A. S. Wan, T. W. Barbee, Jr., R. Cauble, P. Celliers, L. B. Da Silva, J. C. Moreno, P. W. Rambo, G. F. Stone, J. E. Trebes, and F. Weber, Phys. Rev. E **55**, 6293 (1997).
[13]R. A. Bosch, R. L. Berger, B. H. Failor, N. D. Delamater, G. Charatis, and R. L. Kauffman, Phys. Fluids B **4**, 979 (1992).
[14]B. A. Remington, S. W. Haan, S. G. Glendinning, J. D. Kilkenny, D. H. Munro, and R. J. Wallace, Phys. Fluids B **4**, 967 (1992).
[15]C. D. Gregory, J. Howe, B. Loupias, S. Myers, M. M. Notley, Y. Sakawa, A. Oya, R. Kodama, M. Koenig, and N. C. Woolsey, Astrophys. J. **676**, 420 (2008).
[16]R. A. Smith, J. Lazarus, M. Hohenberger, A. Marocchino, J. A. Robinson, J. P. Chittenden, A. S. Moore, E. T. Gumbrell, and M. Dunne, Plasma Phys. Controlled Fusion **49**, B117 (2007).
[17]P. W. Rambo and J. Denavit, Phys. Plasmas **1**, 4050 (1994).
[18]C. Chenais-Popovics, P. Renaudin, O. Rancu, F. Gilleron, J.-C. Gauthier, O. Larroche, O. Peyrusse, M. Dirksmöller, P. Sondhauss, T. Missalla, I. Uschmann, E. Förster, O. Renner, and E. Krousk, Phys. Plasmas **4**, 190 (1997).
[19]R. J. Goldston and P. H. Rutherford, *Introduction to Plasma Physics* (Taylor & Francis, London, 1995).
[20]S. M. Pollaine, R. L. Berger, and C. J. Keane, Phys. Fluids B **4**, 989 (1992).
[21]O. Rancu, P. Renaudin, C. Chenais-Popovics, H. Kawagashi, J.-C. Gauthier, M. Dirksmöller, T. Missalla, I. Uschmann, E. Förster, O. Larroche, O. Peyrusse, O. Renner, E. Krousky, H. Pépin, and T. Shepard, Phys. Rev. Lett. **75**, 3854 (1995).
[22]P. Hough, C. McLoughlin, T. J. Kelly, P. Hayden, S. S. Harilal, J. P. Mosnier, and J. T. Costello, J. Phys. D: Appl. Phys. **42**, 055211 (2009).
[23]M. E. Jones, D. Winske, S. R. Goldman, R. A. Kopp, V. G. Rogatchev, S. A. Bel'kov, P. D. Gasparyan, G. V. Dolgoleva, N. V. Zhidkov, N. V. Ivanov, Yu. K. Kochubej, G. F. Nasyrov, V. A. Pavlovskii, V. V. Smirnov, and Yu. A. Romanov, Phys. Plasmas **3**, 3 (1996).
[24]R. A. Smith, J. Lazarus, M. Hohenberger, A. S. Moore, J. S. Robinson, E. T. Gumbrell, and M. Dunne, Astrophys. Space Sci. **307**, 131 (2007).
[25]S. S. Harilal, C. V. Bindhu, and H.-J. Kunze, J. Appl. Phys. **89**, 4737 (2001).
[26]D. Doria, K. D. Kavanagh, J. T. Costello, and H. Luna, Meas. Sci. Technol. **17**, 670 (2006).
[27]National Institute of Standards and Technology, http://physics.nist.gov/PhysRefData/ASD/.
[28]C. Ursu, S. Gurlui, C. Focsa, and G. Popa, Nucl. Instrum. Methods Phys. Res. B **267**, 446 (2009).
[29]P. Hough, C. McLoughlin, T. J. Kelly, S. S. Harilal, J. P. Mosnier, and J. T. Costello, Appl. Surf. Sci. **255**, 5167 (2009).
[30]Y. Okano, Y. Hironaka, K. G. Nakamura, and K.-I. Kondo, Appl. Phys. Lett. **83**, 1536 (2003).
[31]P. Hough (private communication).
[32]H. Luna, K. D. Kavanagh, and J. T. Costello, J. Appl. Phys. **101**, 033302 (2007).
[33]D. R. Farley, K. G. Estabrook, S. G. Glendinning, S. H. Glenzer, B. A. Remington, K. Shigemori, J. M. Stone, R. J. Wallace, G. B. Zimmerman, and J. A. Harte, Phys. Rev. Lett. **83**, 1982 (1999).